molecular pharmaceutics

Article

Cite This: Mol. Pharmaceutics XXXX, XXX, XXX−XXX

pubs.acs.org/molecularpharmaceutics

Brivanib Exhibits Potential for Pharmacokinetic Drug−Drug Interactions and the Modulation of Multidrug Resistance through the Inhibition of Human ABCG2 Drug Efflux Transporter and CYP450 Biotransformation Enzymes

Jakub Hofman,*[,†] Ales Sorf,[†] Dimitrios Vagiannis,[†] Simona Sucha,[†] Sarah Kammerer,[‡] Jan-Heiner Küpper,[‡] Si Chen,[§] Lei Guo,[§] Martina Ceckova,[†] and Frantisek Staud[†]

[†]Department of Pharmacology and Toxicology, Faculty of Pharmacy in Hradec Kralove, Charles University, Akademika Heyrovskeho 1203, 500 05 Hradec Kralove, Czech Republic

[‡]Institute of Biotechnology, Brandenburg University of Technology Cottbus-Senftenberg, Universitätsplatz 1, 01968 Senftenberg, Germany

[§]Division of Biochemical Toxicology, National Center for Toxicological Research/U.S. FDA, Jefferson, Arkansas 72079, United States

ABSTRACT: Brivanib, a promising tyrosine kinase inhibitor, is currently undergoing advanced stages of clinical evaluation for solid tumor therapy. In this work, we investigated possible interactions of this novel drug candidate with ABC drug efflux transporters and cytochrome P450 (CYP450) drug-metabolizing enzymes that participate in cancer multidrug resistance (MDR) and pharmacokinetic drug−drug interactions (DDIs). First, in accumulation experiments with various model substrates, we identified brivanib as an inhibitor of the ABCB1, ABCG2, and ABCC1 transporters. However, in subsequent combination studies employing 3-(4,5-dimethyl-2-thiazolyl)-2,5-diphenyl-2*H*-tetrazolium bromide proliferation assays in both Madin-Darby canine kidney II (MDCKII) and A431 cellular models, only ABCG2 inhibition was revealed to be able to synergistically potentiate mitoxantrone effects. Advantageous to its possible use as MDR antagonist, brivanib's chemosensitizing properties were not impaired by activity of any of the MDR-associated ABC transporters, as observed in comparative viability assay in the MDCKII cell sublines. In incubation experiments with eight recombinant CYP450s, we found that brivanib potently inhibited CYP2C subfamily members and the CYP2B6 isoform. Finally, in induction studies, we demonstrated that brivanib upregulated *ABCB1* and *CYP1A2* messenger RNA levels in systemic cell models, although this interaction was not significantly manifested at a functional level. In conclusion, brivanib exhibits potential to cause clinically relevant pharmacokinetic DDIs and act as a modulator of ABCG2-mediated MDR. Our findings might be used as an important background for subsequent in vivo investigations and pave the way for the safe and effective use of brivanib in oncological patients.

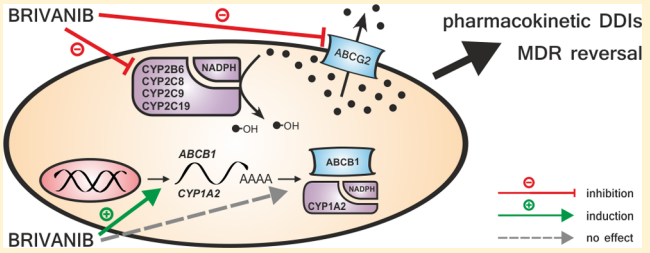

KEYWORDS: *brivanib, ABC drug efflux transporter, cytochrome P450, multidrug resistance, drug−drug interaction*

1. INTRODUCTION

Cancer represents a major human health problem and is expected to surpass cardiovascular diseases as the leading cause of death in the near future.[1] In addition to the considerable progress in surgery and radiotherapy, anticancer pharmacotherapy is dramatically evolving within cancer treatment approaches, providing new hope for cancer patients. Novel targeted drugs have revolutionized cancer therapy due to their selective nature reflected by less toxicity compared with standard cytotoxic agents.[2] Brivanib alaninate, an orally available prodrug of brivanib (Figure 1), is a dual inhibitor of fibroblast growth factor- and vascular endothelial growth factor receptor kinases.

Originally developed by Bristol-Myers Squibb, this small-molecule-targeted drug has been clinically evaluated for the treatment of various solid tumors, including hepatocellular carcinoma and non-small cell lung cancer (NSCLC).[3] Although promising results were reported in phase I and II trials, brivanib did not outperform sorafenib in global phase III clinical trials,[4,5] and further clinical development was halted in Western countries. However, the considerable clinical outcomes more specifically obtained in Asian populations and the

Received: March 29, 2019
Revised: September 20, 2019
Accepted: October 8, 2019

DOI: 10.1021/acs.molpharmaceut.9b00361
Mol. Pharmaceutics XXXX, XXX, XXX−XXX

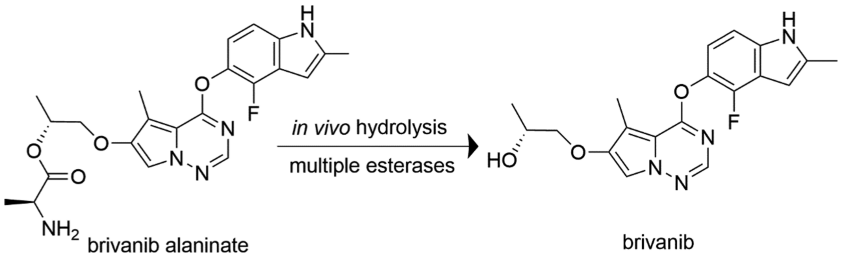

Figure 1. Schematic depiction of brivanib activation in vivo.

economic aspects led to the transfer of its license to a Chinese biopharmaceutical company (Zai Lab). Brivanib is currently being developed for the Chinese drug market (recruiting phase II study with ClinicalTrials.gov Identifier NCT03516071); it is believed that it will become an affordable alternative to sorafenib, which is not widely available in China due to a lack of coverage by health insurance.[6]

ABC [adenosine 5′-triphosphate (ATP)-binding cassette] drug efflux transporters constitute a large group of membrane-embedded carriers that are functionally expressed mainly in organs regulating absorption, distribution, and elimination of drugs (intestine, placenta, testes, brain, liver, and kidney). These carriers actively extrude a palette of structurally diverse xenobiotic compounds, including drugs and their metabolites, out of cells. As implicated by their localization, ABC drug efflux transporters play an important protective role by diminishing absorption and distribution while forcing the excretion of drugs that can cause harmful effects to bodily tissues. These processes considerably influence the general pharmacokinetic behaviors of transporter substrates and can cause clinically relevant pharmacokinetic drug−drug interactions (DDIs) when the transporters are inhibited or induced.[7] The cytochrome P450 (CYP450) superfamily is another critically important component in the pharmacokinetic detoxification unit that closely cooperates with ABC drug efflux transporters in tissue protection. CYP450s convert lipophilic parent drugs into reactive metabolites, thus enhancing their conjugation with endogenous molecules as well as their subsequent excretion from the body. CYP450s are also recognized as crucial sites for pharmacokinetic DDIs that can result in either increased toxicity or decreased efficacy of a victim drug.[8] With respect to this fact, investigation of the interactive potential of new drugs is strongly recommended by drug regulatory authorities.[9]

Apart from their vital roles in xenobiotic tissue protection, several ABC drug efflux transporters and CYP450 biotransformation enzymes are overexpressed in tumors and diminish the accumulation of chemotherapeutic agents by either pumping the drugs out of the cell or through drug deactivation, respectively, thus causing pharmacokinetic multidrug resistance (MDR). To date, ABCG2 (breast cancer resistance protein), ABCB1 (P-glycoprotein), and ABCC1 (multidrug resistance-associated protein 1) have been demonstrated to be able to develop MDR at both in vitro and in vivo levels.[10,11] In contrast to transporters, only few studies investigating the roles of CYP450s in the phenomenon of pharmacokinetic MDR have been reported. For example, decreased anticancer effects of vincristine, docetaxel, and paclitaxel have been suggested to be mediated by the metabolism through CYP2C8 and CYP3A4/5 isoforms in cancer cells.[12−14] CYP3A4 was experimentally proven to significantly attenuate the cytotoxic effects of docetaxel (our unpublished data). In previous clinical trials aiming to circumvent transporter-mediated resistance, several noncytotoxic ABC transporter inhibitors have been combined with standard cytostatic drugs; however, despite promising initial results, clinical development of these compounds has been discontinued in later stages because of low efficiency and/or provoking systemic toxic response.[15] Nevertheless, targeting pharmacokinetic MDR mechanisms remained an attractive method for treatment approaches. Currently, the combination of novel MDR modulators from the group of targeted drugs with classical cytostatic agents is believed to become a new therapeutic option for resistant tumors.[16,17] In our lab, we have recently demonstrated that several novel cyclin-dependent kinase inhibitors can effectively modulate cytostatic MDR via interactions with ABCB1, ABCG2, and/or ABCC1.[18−22] These dual-mechanism properties could be beneficially utilized in various combination regimens following in vivo evaluation.

While the pharmacodynamic behavior of brivanib has been extensively investigated, the knowledge of its pharmacokinetic profile is fragmentary. In this work, we aimed to describe the ability of brivanib to inhibit various ABC transporters and CYP450s that play roles in both pharmacokinetic MDR and DDIs. We subsequently evaluated the possible utilization of the observed interactions to overcome resistance to standard cytostatic drugs. In addition to investigating brivanib's chemosensitization effects, we also evaluated its possible opposing role in pharmacokinetic MDR, i.e., whether brivanib might be a victim of this phenomenon. Finally, we tracked the effect of brivanib on messenger RNA (mRNA) levels and the functional activities of the examined transporters and enzymes. Our in vitro work provides the first comprehensive overview of the potential of brivanib to act as a perpetrator of pharmacokinetic DDIs and its role in pharmacokinetic MDR.

2. MATERIALS AND METHODS

2.1. Reagents and Chemicals. Brivanib was purchased from Selleckchem (Houston, TX). Hoechst 33342 and rhodamine 123 were obtained from Sigma-Aldrich (St. Louis, MO), and calcein AM was from Thermo Fisher Scientific (Waltham, MA). Dimethyl sulfoxide (DMSO), mitoxantrone, daunorubicin, 3-(4,5-dimethyl-2-thiazolyl)-2,5-diphenyl-2*H*-tetrazolium bromide (MTT), and cell culture-related reagents were supplied by Sigma-Aldrich. Hepatocyte culture medium and hepatocyte high performance medium were obtained from Upcyte Technologies (Hamburg, Germany). Opti-MEM was purchased from Gibco BRL Life Technologies (Rockville, MD). LY335979 (zosuquidar) was obtained from Toronto Research Chemicals (North York, ON, Canada). MK-571 (verlukast) and Ko143 were purchased from Enzo Life Sciences (Farmingdale, NY). Vivid CYP450 screening kits specific for CYP1A2, CYP2B6, CYP2C8, CYP2C9, CYP2C19,

DOI: 10.1021/acs.molpharmaceut.9b00361
Mol. Pharmaceutics XXXX, XXX, XXX−XXX

CYP2D6, CYP3A4, or CYP3A5 isoforms were from Thermo Fisher Scientific. The CYP450 model inducers rifampicin (CYP3A4), omeprazole (CYP1A2), and phenobarbital (CYP2B6) and CYP450 inhibitors α-naphthoflavone (CYP1A2), miconazole (CYP2B6 and CYP2C19), montelukast (CYP2C8), sulfaphenazole (CYP2C9), quinidine (CYP2D6), and ketoconazole (CYP3A4 and CYP3A5) were from Sigma-Aldrich. The P450-Glo CYP3A4 assay and screening system with Luciferin-IPA, P450-Glo CYP1A2 induction/inhibition assay, CellTiter-Glo luminescent cell viability assay, and CellTiter-Glo 2.0 cell viability assay were from Promega (Madison, WI). The Pierce bicinchoninic acid (BCA) protein assay kit was obtained from Thermo Fisher Scientific. The TRI reagent was from Molecular Research Center (Cincinnati, OH). The InnuPREP RNA mini kit was purchased from Analytik Jena (Jena, Germany). TaqMan quantitative real-time polymerase chain reaction (qRT-PCR) systems specific for *ABCB1*, *ABCG2*, and *ABCC1*, gb Easy PCR master mix and the gb reverse transcription kit were purchased from Generi Biotech (Hradec Kralove, Czech Republic). DNase I, reaction buffer with $MgCl_2$, and 50 mM ethylenediaminetetraacetic acid as well as oligo $(dT)_{18}$ primers, 10 mM deoxynucleoside triphosphates and revert aid reverse transcriptase for DNase digestion and complementary DNA (cDNA) synthesis, respectively, were from Thermo Fisher Scientific. qRT-PCR for the analysis of *CYP1A2*, *CYP2B6*, and *CYP3A4* expression was performed with a Maxima Probe qPCR master mix (Thermo Fisher Scientific) and EvaGreen (Biotium, Fremont, CA).

2.2. Cell Culture. The Madin-Darby canine kidney (MDCKII) cell sublines stably overexpressing human transporters ABCG2 (MDCKII-ABCG2), ABCB1 (MDCKII-ABCB1), or ABCC1 (MDCKII-ABCC1) together with MDCKII-parent (MDCKII-par) cell line were supplied by Dr. Alfred Schinkel (The Netherlands Cancer Institute, Amsterdam, The Netherlands). The A431-parent cells derived from human epidermoid carcinoma and its cytostatic-resistant ABCB1-, ABCG2-, and ABCC1-overexpressing variants A431-ABCB1, A431-482R/MX100 (abbreviated as A431-ABCG2 in this work), and A431-ABCC1, respectively, were kindly provided by Dr. Balasz Sarkadi (Hungarian Academy of Sciences, Budapest, Hungary).[23] The construction and characterization of HepG2-CYP3A4, human liver carcinoma HepG2 cells stably transduced with human CYP3A4, is as described previously.[24] Human A549 cells derived from NSCLC adenocarcinoma were obtained from the American Type Culture Collection (ATCC, Manassas, VA). MDCKII, A431, HepG2, and A549 cells were cultivated in high-glucose Dulbecco's modified Eagle's medium (DMEM) enriched with 10% fetal bovine serum (FBS). The human colorectal adenocarcinoma Caco-2 and human NSCLC carcinoma NCI-H1299 cell lines were purchased from ATCC. Caco-2 cells were cultivated in high-glucose DMEM enriched with 10% FBS and 1% nonessential amino acids. NCI-H1299 were grown in Roswell Park Memorial Institute-1640 supplemented with 10% FBS, 10 mM 4-(2-hydroxyethyl)-1-piperazineethanesulfonic acid, and 1 mM sodium pyruvate. The human colorectal adenocarcinoma LS174T cell line was purchased from the European Collection of Cell Cultures (Salisbury, U.K.); the cells were cultivated in Eagle's minimal essential medium containing 10% FBS, 1% nonessential amino acids, and 2 mM glutamine. The HepaFH3 hepatocyte cell line was generated using the upcyte technology and characterized as described previously.[25] Second-generation upcyte hepatocytes were derived from another donor (no. 653-03) and prepared by Upcyte Technologies (Hamburg, Germany).[26] Both proliferating primary-like hepatocyte sublines were cultivated in hepatocyte culture medium, while hepatocyte high performance medium was utilized for experiments. Both standard culturing and experiments were performed in media without antibiotics under common conditions (humidified atmosphere containing 5% CO_2, 37 °C). The cell cultures were checked for possible mycoplasma infection before and at the end of experiments. DMSO was used as a vehicle for brivanib at concentrations ≤0.5%. No-vehicle controls were applied in cellular accumulation and MTT proliferation experiments; the effects of 0.5% DMSO (<2% change of particular no-vehicle control values) were insignificant with respect to the tested parameters. When DMSO had significant effects on the tested parameters (in the CYP3A4 inhibitory assay in intact cells as well as in induction studies), a vehicle control approach was employed to compensate for the effects of DMSO.

2.3. Cellular Accumulation Assay with Noncytotoxic Substrates. Briefly, MDCKII-ABCG2, MDCKII-ABCB1, MDCKII-ABCC1, and MDCKII-parent cells ($5.0–6.0 \times 10^4$ cells per well) were seeded on transparent 96-well plates. After 24 h, the cells were rinsed twice with 1× phosphate-buffered saline (PBS) and the solutions of Opti-MEM containing either brivanib (1, 5, 10, 25, and 50 μM) or model inhibitors (1 μM Ko143, 1 μM LY335979, and 25 μM MK-571 for ABCG2, ABCB1, and ABCC1, respectively) were added. The cells were incubated for 10 min under standard conditions, and then 8 μM Hoechst 33342 (ABCG2/ABCB1 probe substrate) or 2 μM calcein AM (ABCC1 substrate) in Opti-MEM was added promptly to all of the variants with the exception of blank samples, and the probe substrate levels in cells were recorded using a microplate reader (Infinite M200 Pro, Tecan, Männedorf, Switzerland). Fluorescence signals (excitation/emission of 350/465 nm for Hoechst 33342 and 485/535 nm for calcein AM) were gained in kinetic bottom mode at 60 s intervals for 30 min.

2.4. Cellular Accumulation Assay with Cytostatic Substrates. MDCKII-ABCG2, MDCKII-ABCB1, MDCKII-ABCC1, and MDCKII-parent cells (1.5×10^5 cells per well) were seeded on 12-well culture plates. After 24 h, the cells were rinsed with 1× PBS, which was followed by the addition of solutions of Opti-MEM containing either brivanib (0.1, 1, 5 10, 25, and 50 μM) or selective control inhibitors (1 μM Ko143, 1 μM LY335979, and 25 μM MK-571 for ABCG2, ABCB1, and ABCC1, respectively). The plates were incubated under standard conditions for 10 min. Subsequently, Opti-MEM solutions of mitoxantrone (ABCG2 probe substrate) or daunorubicin (ABCC1/ABCB1 substrate) were added promptly to the wells (except for background samples) reaching final concentrations of 1 or 2 μM, respectively. The cells were incubated under standard conditions for 1 h. The accumulation/efflux phase was then stopped by placing plates on ice, rinsing cells twice with ice-cold 1× PBS, and adding lysis buffer composed of 150 mM NaCl, 25 mM Tris, and 1% Triton X-100. After automatized shaking (30 min, room temperature), the lysates were vigorously resuspended, harvested, and centrifuged (10 000 rpm, 5 min). Supernatants in 100 μL volume were pipetted into a black 96-well plate, and the intracellular levels of cytostatic substrates were determined fluorometrically (excitation/emission of 640/670 nm for mitoxantrone and 490/565 nm for daunorubicin) using a

DOI: 10.1021/acs.molpharmaceut.9b00361
Mol. Pharmaceutics XXXX, XXX, XXX−XXX

microplate reader (Infinite M200 Pro, Tecan). The Pierce BCA protein assay kit was employed to quantify the protein concentrations in samples. The relative fluorescence unit (RFU) values obtained in the assessments of cytostatic substrate levels were normalized to the protein concentrations.

2.5. Determination of the Inhibition of Human Recombinant CYP450s. CYP3A4, an enzyme participating in docetaxel resistance, and other CYP450 isoforms (i.e., CYP1A2, CYP3A4, CYP3A5, CYP2B6, CYP2C8, CYP2C9, CYP2C19, and CYP2D6) recommended for inhibition screening by the U.S. Food and Drug Administration (U.S. FDA) and European Medicines Agency (EMA) were tested in these experiments. Inhibitory properties of brivanib were evaluated using Vivid CYP450 screening kits, which contained microsomal fractions extracted from insect cells overexpressing particular human CYP450 isozymes. Experiments were performed according to the manufacturer's instructions with minor modifications. The gradual production of metabolites was determined fluorometrically in a kinetic mode (1 min interval for 60 min) using a microplate reader (Infinite M200 Pro, Tecan). The 15 min incubation intervals selected for data evaluation and concentrations of enzymes were within the linear portion of the particular reaction velocity curves. The effects of DMSO on enzyme activities were eliminated by predilution of brivanib in DMSO such that 0.5% DMSO was introduced at the tested concentrations. 0.5% DMSO was also present in all controls (0 and 100% activity controls, model inhibitors). Model inhibitors were chosen according to the recommendation of the manufacturer; the compounds were used as positive inhibitory controls.

2.6. CYP3A4 Inhibitory Assay in Intact Cells. A cell-based method for testing CYP3A4 inhibition was developed using a P450-Glo CYP3A4 assay and screening system with Luciferin-IPA together with the CellTiter-Glo luminescent cell viability assay. HepG2-3A4 cells were seeded on a transparent 96-well plate at a density of 8.0×10^4 cells per well and cultured for 24 h. The cells were rinsed once with 1× PBS and exposed to solutions of Opti-MEM containing DMSO (0.01, 0.1, and 0.4%; vehicle controls), brivanib (1, 10, and 40 μM), or 10 μM ketoconazole used as model-specific inhibitor and preincubated for 10 min at 37 °C and 5% CO_2. Luciferin-IPA substrate at a final concentration of 2 μM was added rapidly to all wells except for the background samples, and the plate was incubated for 45 min. The cells were placed on ice after incubation and a portion of the cells' culture media was transferred to an opaque white 96-well plate and mixed with Luciferin detection reagent at a ratio of 1:1 (v/v). The resulting mixture was incubated at room temperature for 20 min followed by luminescence measurements (integration time: 250 ms) using a microplate reader (Infinite M200 Pro, Tecan). The remaining cell culture media was removed, 35 μL of pure Opti-MEM was added, and plate was equilibrated at room temperature for 30 min. Subsequently, 25 μL of CellTiter-Glo reagent was added to the cells and the plate was placed on an orbital shaker for 2 min to induce cell lysis. After 10 min of incubation at room temperature, 50 μL of the resulting mixture was transferred to an opaque white 96-well plate and luminescent signals corresponding to cell viability were read under the same conditions as in the previous step. Data from metabolic testing were normalized to viability values to compensate for possible inaccuracies caused by nonuniformity in cell growth or for false-positive results due to drug cytotoxicity. Values from particular brivanib concentrations were normalized to the values of the respective vehicle controls. The method was thoroughly optimized (procedure, cell seeding density, incubation intervals, substrate concentration, and check of possible interference of luminescent signal with drug or drug metabolite) in advance of the experiments.

2.7. MTT Viability Assay. MDCKII-ABCG2, MDCKII-ABCB1, MDCKII-ABCC1, and MDCKII-par (1.3×10^4 cells per well); A431-ABCG2 (1.0×10^4 cells per well); A431-ABCB1, A431-ABCC1, and A431-par (1.2×10^4 cells per well); LS174T (5.0×10^4 cells per well); Caco-2 (2.0×10^4 cells per well); NCI-H1299 (0.75×10^4 cells per well); and A549 (0.80×10^4 cells per well) cells were seeded on 96-well culture plates. After 24 h of cultivation, the medium was removed and freshly prepared solutions of the evaluated drugs or drug combinations were added to the cells. The cells were incubated with drugs for 48 h under common conditions. Afterward, the medium was removed and the cells were rinsed once with 1× PBS, which was followed by the addition of 1 mg/mL MTT in Opti-MEM. Then, the cells were incubated for 1 h (MDCKII cell lines) or 45 min (the other cell lines). The MTT solution was removed and the proper lysis of cells by DMSO was accomplished via automatized shaking for 10 min. Absorbance in samples was determined at 570 and 690 nm using a microplate reader (Infinite M200 Pro, Tecan). The values obtained at 690 nm (background) were subtracted from the values measured at 570 nm (detecting MTT formazan product). To normalize the absorbance values, the absorbance of samples with drug-free medium was used as 100% viability. The values of 0% viability were from cells exposed to medium containing 10% DMSO. The MTT viability assay was employed to: (1) evaluate the ability of brivanib to overcome MDR in drug combination studies, (2) determine the influence of functional expression of ABC transporters on the antiproliferative effect of brivanib in MDCKII cells, and (3) choose the proper brivanib concentration to be tested in transporter-oriented mRNA gene expression assays.

2.8. Drug Combination Studies. Drug combination experiments were performed in nonconstant ratio setup as described previously.[27] The A431 and MDCKII cell lines were seeded at the densities described above on 96-well culture plates 24 h before experiment. The medium was removed, and freshly prepared solutions of brivanib alone at different concentrations or a range of probe anticancer drug (mitoxantrone, daunorubicin) concentrations with or without 15 or 20 μM brivanib were added to the cells. After 48 h incubation, cell proliferation was assessed using MTT assay (see method description above). The proliferation data were transformed to F_A (fraction of cells affected; F_A = 100 − viability) values, and the outcomes of drug combinations were determined via the combination index (CI) method of Chou−Talalay. This method based on the median-effect equation offers the possibility to precisely define the outcome of the combination of two or more drugs. Using the CompuSyn 3.0.1 software (ComboSyn Inc., Paramus, NJ), the dose−F_A data for brivanib alone, daunorubicin/mitoxantrone alone, and their combinations were analyzed by following a nonconstant ratio algorithm yielding CI values for each dose point. Based on the CI, the combination effects are considered as either antagonistic (CI > 1.1), additive (CI = 0.9−1.1) or synergistic (CI < 0.9). For more details on the theory, design of experiments and computer-based simulation of the combina-

DOI: 10.1021/acs.molpharmaceut.9b00361
Mol. Pharmaceutics XXXX, XXX, XXX−XXX

tion drug effects employing the CI method, see the review by Chou.[28]

2.9. mRNA Expression Studies. Although both transporter- and enzyme-oriented gene expression studies were performed using qRT-PCR analysis of mRNA levels, the methodologies used vary considerably; therefore, they are described separately.

For transporter analysis, an appropriate concentration of brivanib was selected based on the results of MTT viability assay (see above). For mRNA expression studies, LS174T, Caco-2, NCI-H1299, or A549 (100×10^4, 50×10^4, 18×10^4, or 24×10^4 cells per well, respectively) cells were seeded on 12-well plates. After 24 h incubation, the medium was removed and solutions of 10 μM brivanib or 25 μM rifampicin or 0.1% DMSO (vehicle control) were added to the cells. Sampling was performed using the TRI reagent at 24 and 48 h intervals, total RNA from samples was then extracted and purified based on the manufacturer's protocol. The quality and integrity of RNA samples were checked by agarose gel electrophoresis. Reverse transcription was performed using the gb reverse transcription kit transcribing 1000 ng of RNA per sample. mRNA levels of *ABCG2, ABCB1*, and *ABCC1* were quantified with TaqMan qRT-PCR systems and the gb Easy PCR master mix in 384-well plates (20 ng of cDNA was amplified per reaction). The analysis of the changes in mRNA levels of tested ABC transporters was performed by employing the $2^{-\Delta\Delta Ct}$ method using the geometric mean of *B2M* and *HPRT1* housekeeping genes as an internal control. The qRT-PCR experiments were run on a QuantStudio 6 thermocycler (Life Technologies, Carlsbad, CA) applying an initial single denaturation at 95 °C for 3 min and 40 cycles consisting of 95 °C for 10 s and 60 °C for 20 s.

In the CYP450 analysis, the effect of brivanib on HepaFH3/upcyte cell viability was also assessed before gene expression experiments to select a correct concentration. Briefly, HepaFH3 and upcyte hepatocytes were seeded at a density of 12 500 cells per well on collagen I-coated 96-well plates 4 days before starting the experiment. Then, the medium was removed and freshly prepared medium containing different concentrations of brivanib was added to the cells. The cells were incubated for 72 h with daily medium exchange including brivanib, and viability was analyzed with the CellTiter-Glo 2.0 cell viability assay according to the manufacturer's protocol. The luminescence was measured using a microplate reader (FLUOstar Omega, BMG Labtech, Ortenberg, Germany). For the gene expression studies, HepaFH3 and upcyte hepatocytes were seeded on collagen I-coated 12-well plates (1.6×10^5 cells per well) 4 days before the experiment to reach full confluence. Subsequently, the medium was removed and freshly prepared solutions of 10 μM brivanib, 50 μM omeprazole, 750 μM phenobarbital, 25 μM rifampicin, or 0.1% DMSO (vehicle control) were added to the cells. Total RNA was isolated after 72 h and the medium was changed daily, including the respective substances using the InnuPREP RNA mini kit according to the manufacturer's instructions. The total RNA content was measured using a NanoDrop, and 3 μg of RNA per sample was subjected to DNase I digestion followed by agarose gel electrophoresis for the verification of RNA integrity. Reverse transcription was conducted using the revert aid reverse transcriptase and 1 μg of DNase-digested RNA. The mRNA levels of *CYP1A2* (forward, 5′-TCGTAAACCAGTGGCAGGT-3′, and reverse, 5′-GGTCAGGTCGACTTTCACG-3′), *CYP2B6* (forward, 5′-CTCTCCATGACCCACACT-3′, and reverse, 5′-CTCTCAGAGGCAGGAAGTTG-3′), and *CYP3A4* (forward, 5′-GTGGGGCTTTTATGATGGTCA-3′, and reverse, 5′-GCCTCAGATTTCTCACCAACACA-3′) were determined using the Maxima Probe qPCR master mix and EvaGreen in 96-well plates following the manufacturer's protocol (0.3 μL of cDNA was amplified per reaction). The analysis of the changes in mRNA levels of tested CYP enzymes was performed by employing the $2^{-\Delta\Delta Ct}$ method using the geometric mean of *GAPDH* (forward, 5′-TGCACCACCAACTGCTTAGC-3′, and reverse, 5′-GGCATGGACTGTGGTCATGAG-3′) and *SDHA* (forward, 5′-CGAACGTCTTCAGGTGCTTT-3′, and reverse, 5′-AAGAACATCGGAACTGCGAC-3′) housekeeping genes as an internal control. qRT-PCR was performed on a CFX96 Touch Real-Time PCR detection system (Bio-Rad, Hercules, CA) with an initial denaturation at 95 °C for 3 min and 45 cycles consisting of 95 °C for 10 s, 62 °C for 10 s, and 72 °C for 30 s, followed by melting curve analysis.

2.10. ABCB1 and CYP1A2 Activity Assays. The impact of positive results obtained in the gene induction studies was evaluated at the functional level using ABCB1 and CYP1A2 activity assays.

For the ABCB1 activity assay, LS174T cells were seeded at a density of 7.5×10^4 cells per well on 96-well plates and cultivated for 24 h. At time 0, medium was replaced with fresh medium containing 10 μM brivanib or 25 μM rifampicin or 0.1% DMSO (vehicle control). Sampling was performed at 24, 48, and 72 h intervals; variants with or without drug washout 6 h before sampling were tested for brivanib. Medium was removed and the cells were washed with 1× PBS. Rhodamine 123 (specific ABCB1 probe substrate) in Opti-MEM at a final concentration of 10 μM was added promptly to all of the variants with the exception of blank wells. After 30 min of incubation, the plates were placed on ice, the media was removed, and the cells were washed twice with ice-cold 1× PBS. The cells were lysed in lysis buffer (25 mM Tris, 150 mM NaCl, and 1% Triton X-100, pH 7.8) in an incubator for 30 min. The lysates from three wells were pooled and subjected to centrifugation (12 000*g* for 5 min) to obtain pure lysates free of cellular debris. The fluorescence (excitation/emission wavelengths of 490/525 nm) of the lysates was assessed in black 96-well plates using a microplate reader (Infinite M200 Pro, Tecan). The protein contents of the cell lysates were assessed by employing Pierce BCA protein assay kit. The RFU values obtained in the assessment of rhodamine 123 levels were normalized to the protein concentrations.

For the CYP1A2 activity assay, HepaFH3 and upcyte hepatocytes were seeded on collagen I-coated 96-well plates (4.35×10^4 cells per well) 4 days before the experiment to reach full confluence. Subsequently, the medium was removed and solutions of 10 μM brivanib, 50 μM omeprazole, or 0.1% DMSO (vehicle control) were added to the cells. The cells were incubated for 72 h with daily medium exchange including the tested compounds. The P450-Glo CYP1A2 induction/inhibition assay was performed according to the manufacturer's protocol in 96-well plates. Briefly, cells and blank medium controls were incubated with 50 μL of substrate solution in 1× PBS for 60 min at 37 °C. Then, 25 μL of the resulting solutions were transferred to a white-walled 96-well plate and incubated for 20 min at room temperature in the dark with 25 μL of detection reagent, after which luminescence signals were measured using a FLUOstar Omega microplate reader. To normalize values to the seeded cell numbers, the CellTiter-Glo

DOI: 10.1021/acs.molpharmaceut.9b00361
Mol. Pharmaceutics XXXX, XXX, XXX−XXX

2.0 cell viability assay was performed according to manufacturer's protocol after incubation of the cells with substrate solution from the P450-Glo assay. Shortly thereafter, 25 μL of CellTiter-Glo 2.0 reagent was added to 25 μL of the remaining substrate solution per well. The plates were shaken at 350 rpm for 2 min and incubated for 10 min at room temperature in the dark. The mixtures were transferred to a white-walled 96-well plate and luminescence signals were measured using a microplate reader as described above.

2.11. Statistical Analysis. The obtained results were statistically evaluated using GraphPad Prism software version 7.03 (GraphPad Software Inc., La Jolla, CA). The one-way analysis of variance (ANOVA) followed by Dunnett's post hoc test or a two-tailed unpaired *t*-test was used to assess statistical significance, while $p < 0.05$ was considered statistically significant. GraphPad Prism software was further used to generate half-maximal inhibitory concentration (IC_{50}) values while applying nonlinear regression analysis using $1/SD^2$ weighting method. All experiments were performed as three independent repetitions with biological triplicates for each repetition.

3. RESULTS

3.1. Brivanib Increases the Intracellular Accumulation of Noncytotoxic Substrates in MDCKII-ABCB1, MDCKII-ABCG2, and MDCKII-ABCC1 Cells. In the initial experiments, we investigated whether brivanib could affect the accumulation of probe noncytotoxic substrates in the MDCKII sublines. Brivanib significantly inhibited all three examined ABC drug efflux transporters with different potencies. Hoechst 33342 efflux mediated by ABCB1 was moderately inhibited with an IC_{50} of 18.4 μM, while maximal inhibition was equal to 63% of the LY335979 effect (Figure 2A). Brivanib strongly inhibited ABCG2 activity with an IC_{50} of 6.98 μM and reached the potency of the model inhibitor Ko143 (Figure 2B). In contrast, affinity toward ABCC1 was very low; a statistically significant increase in calcein AM accumulation was only recorded at the 25 μM concentration of brivanib, with the maximal inhibitory effect equal to only 19% of the MK-571 effect (Figure 2C). As expected, no significant changes were detected in the control MDCKII-par cells (Figure 2A–C).

3.2. Effect of Brivanib on the Intracellular Accumulation of Cytotoxic Substrates in the MDCKII Sublines. The cytostatic substrates mitoxantrone and daunorubicin were used to confirm the results from the initial investigation with noncytotoxic substrates. Since these cytotoxic drugs were subsequently employed in MDR reversal studies, the outcomes of the experiments also served to clarify whether brivanib had the potential to be applied as an MDR modulator.

Similar to the results obtained with the MDCKII sublines (Figure 2), brivanib exhibited more than 4-fold higher inhibitory potency toward ABCG2 compared to ABCB1 as reflected by the IC_{50} values of 9.61 and 44.1 μM, respectively. The maximal ABCB1 and ABCG2 inhibitory effects reached by brivanib in our setup were equal to 55 and 68% of LY335979 and Ko143, respectively (Figure 3A,B). In the daunorubicin accumulation assay, brivanib showed a relatively potent inhibition of ABCC1 efflux activity with an IC_{50} of 25.3 μM and a maximal effect of 72% compared to MK-571 (Figure 3C). No statistically significant changes were observed in the control MDCKII-par cells (Figure 3A–C).

3.3. Modulation of ABC Transporter-Mediated MDR by Brivanib. Here, we evaluated whether the inhibitory properties of brivanib toward ABCG2, ABCB1, and ABCC1 could be exploited to circumvent MDR to the established resistance victim substrates mitoxantrone and daunorubicin. This hypothesis was first tested in MDCKII cells and then a

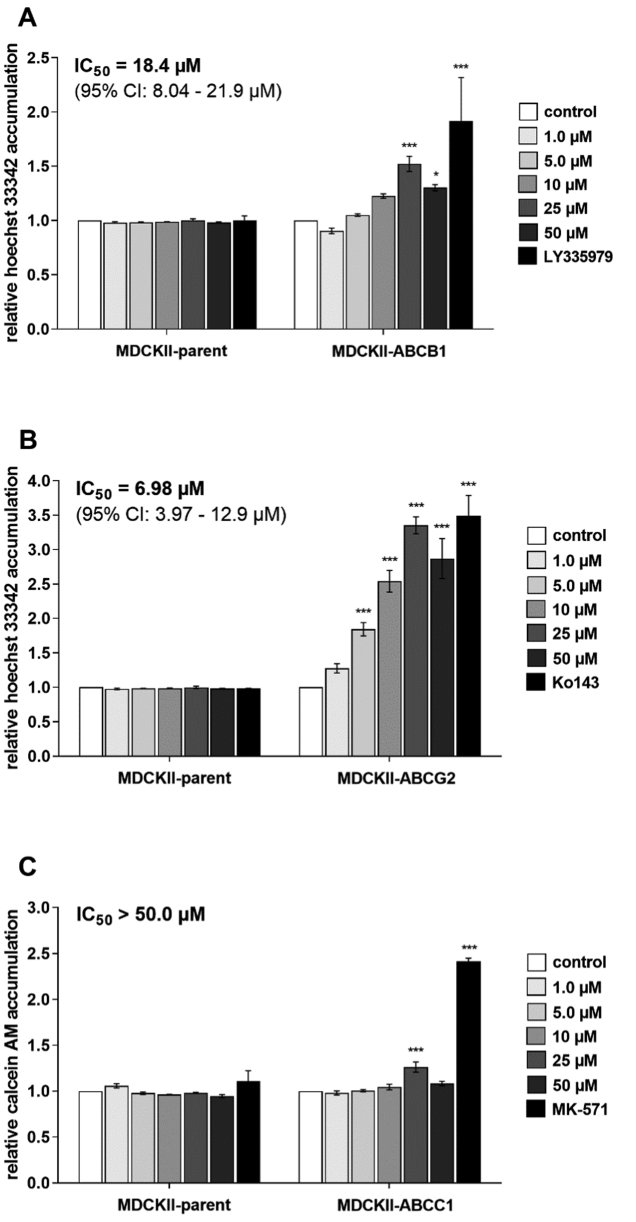

Figure 2. Effect of brivanib on the intracellular accumulation of fluorescent noncytotoxic substrates in (A) MDCKII-ABCB1, (B) MDCKII-ABCG2, and (C) MDCKII-ABCC1 cells. The results obtained with control MDCKII-par cells are shown for each variant. The inhibitors 1 μM Ko143, 1 μM LY335979, and 25 μM MK-571 were used as inhibitory controls; the chosen concentrations were experimentally verified to show the maximum possible inhibition of particular transporters. The cells were incubated with tested drug or control inhibitors for 10 min, after which 2 μM calcein AM or 8 μM Hoechst 3342 was added, and the probe substrate levels were determined in a kinetic setup for 30 min. Data are expressed as mean ± standard deviation (SD) obtained from three independent experiments with biological triplicates for each repetition. IC_{50} values were determined as absolute values considering the model inhibitor response as 100% inhibitory effect. Statistical analysis was performed using one-way ANOVA followed by Dunnett's post hoc test (*$p < 0.05$ and ***$p < 0.001$ compared to the control).

DOI: 10.1021/acs.molpharmaceut.9b00361
Mol. Pharmaceutics XXXX, XXX, XXX−XXX

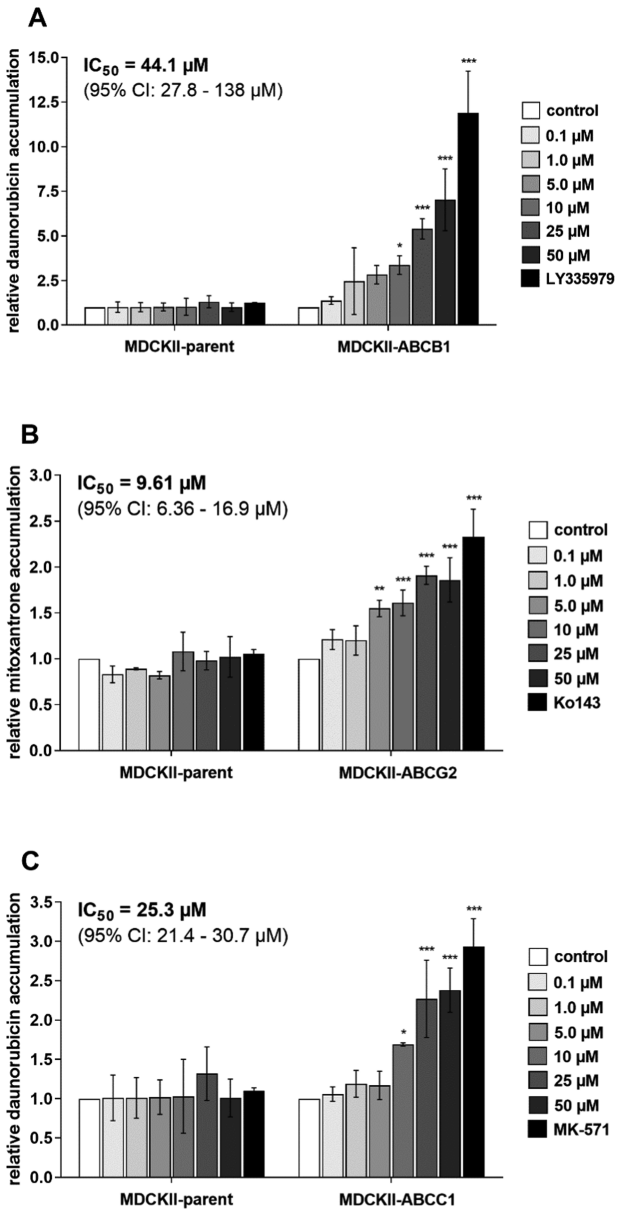

Figure 3. Influence of brivanib on the intracellular accumulation of fluorescent cytotoxic substrates in (A) MDCKII-ABCB1, (B) MDCKII-ABCG2, and (C) MDCKII-ABCC1 cells. Values obtained with control MDCKII-par cells are presented for each variant. The inhibitors 1 μM Ko143, 1 μM LY335979, and 25 μM MK-571 were used as inhibitory controls; the chosen concentrations were shown to yield the maximum possible inhibition of particular transporters. The cells were incubated with tested drug or control inhibitors for 10 min, after which 1 μM mitoxantrone or 2 μM daunorubicin was added. Accumulation was stopped at 1 h interval, the cells were lysed, and the probe substrate levels were determined fluorometrically. Obtained values were subsequently normalized to the protein contents. Data are expressed as mean ± SD obtained from three independent experiments with biological triplicates for each repetition. The IC_{50} values were assessed as absolute values considering the model inhibitor response as 100% inhibitory effect. Statistical analysis was performed using one-way ANOVA followed by Dunnett's post hoc test (*p < 0.05, **p < 0.01, and ***p < 0.001 compared to the control).

similar study was performed in a human model of cytostatic-resistant A431 cell lines. The following three criteria were used for the selection of brivanib concentrations for the MDR modulatory experiments: (1) caused significant transporter inhibition; (2) showed only negligible (<20%) cytotoxicity in the tested cell lines; and (3) are achievable in the plasma of oncological patients receiving a standard dose of 800 mg once daily.[29]

Brivanib partly reversed daunorubicin resistance in MDCKII-ABCB1 cells as observed by significant 2.62-fold IC_{50} shift (Figure 4A and Table 1). Corresponding to its high inhibitory potency toward ABCG2, this drug candidate completely overcame mitoxantrone resistance in ABCG2-overexpressing MDCKII cells (significant IC_{50} shift of 8.60) reaching IC_{50} values of parent cells in the presence of modulator (Figure 4B and Table 1). Although brivanib showed relatively potent inhibition of ABCC1 in the daunorubicin accumulation assay (Figure 3C), it failed to modulate ABCC1-mediated resistance to daunorubicin, as no significant IC_{50} shift was observed in MDCKII-ABCC1 cells after the addition of brivanib (Figure 4C and Table 1). In the A431-ABCB1 cell line, the tested drug did not cause any significant changes in sensitivity to daunorubicin (Figure 4D and Table 1). In contrast, the significant 7.84-fold IC_{50} shift obtained in A431-ABCG2 confirmed the potential of brivanib to act as an effective modulator of ABCG2-mediated resistance to mitoxantrone (Figure 4E and Table 1). Similar to that observed in MDCKII-ABCC1 cells, we detected an insignificant decrease in IC_{50} values following brivanib exposure together with daunorubicin in A431-ABCC1 cells (Figure 4F and Table 1). Finally, insignificant IC_{50} shifts were observed for all combination variants in the control MDCKII-par and A431-par cells (Figure 4A–F and Table 1). In addition, the participation of ABCG2 inhibition in the modulation of mitoxantrone resistance was confirmed using the analysis of results according to Chou–Talalay's combination index method; this widely used method offers a quantitative definition of an additive effect, synergism, or antagonism in drug combination studies. While a predominantly antagonistic effect was observed for the parent cells, the synergistic pattern of the brivanib–mitoxantrone combination was found in ABCG2-overexpressing cells (Figure 5B,E). For MDCKII-ABCB1 and A431-ABCC1, similar trends were observed but only at extremely high or low F_A (fraction of cells affected) values (Figure 5A,F). For the last two remaining variants (MDCKII-ABCC1 and A431-ABCB1), antagonism was recorded across almost the whole F_A range with no significant differences between the transporter-overexpressing and parent cells (Figure 5C,D).

3.4. ABCB1, ABCG2, and ABCC1 Transporters Do Not Confer Resistance to Brivanib. Following the investigation of brivanib's chemosensitization effects, we evaluated its possible opposite role in pharmacokinetic MDR, i.e., whether brivanib might be a victim of this phenomenon. In this study, we compared the sensitivity of parent versus transporter-transduced MDCKII cells exposed to brivanib. Only insignificant differences in brivanib's antiproliferative capacity were recorded between MDCKII-par (IC_{50} = 49.1 μM) and MDCKII-ABCB1 (IC_{50} = 34.4 μM), MDCKII-ABCG2 (IC_{50} = 42.3 μM), or MDCKII-ABCC1 (IC_{50} = 34.8 μM) cells (Figure 6). These results suggest insignificant roles of all three tested transporters in the development of resistance to brivanib.

3.5. Effect of Brivanib on the Activity of Clinically Relevant Recombinant CYP450 Isoenzymes. Inhibition of the recombinant CYP1A2, CYP3A4, CYP3A5, CYP2B6, CYP2C8, CYP2C9, CYP2C19, and CYP2D6 isoforms was

DOI: 10.1021/acs.molpharmaceut.9b00361
Mol. Pharmaceutics XXXX, XXX, XXX–XXX

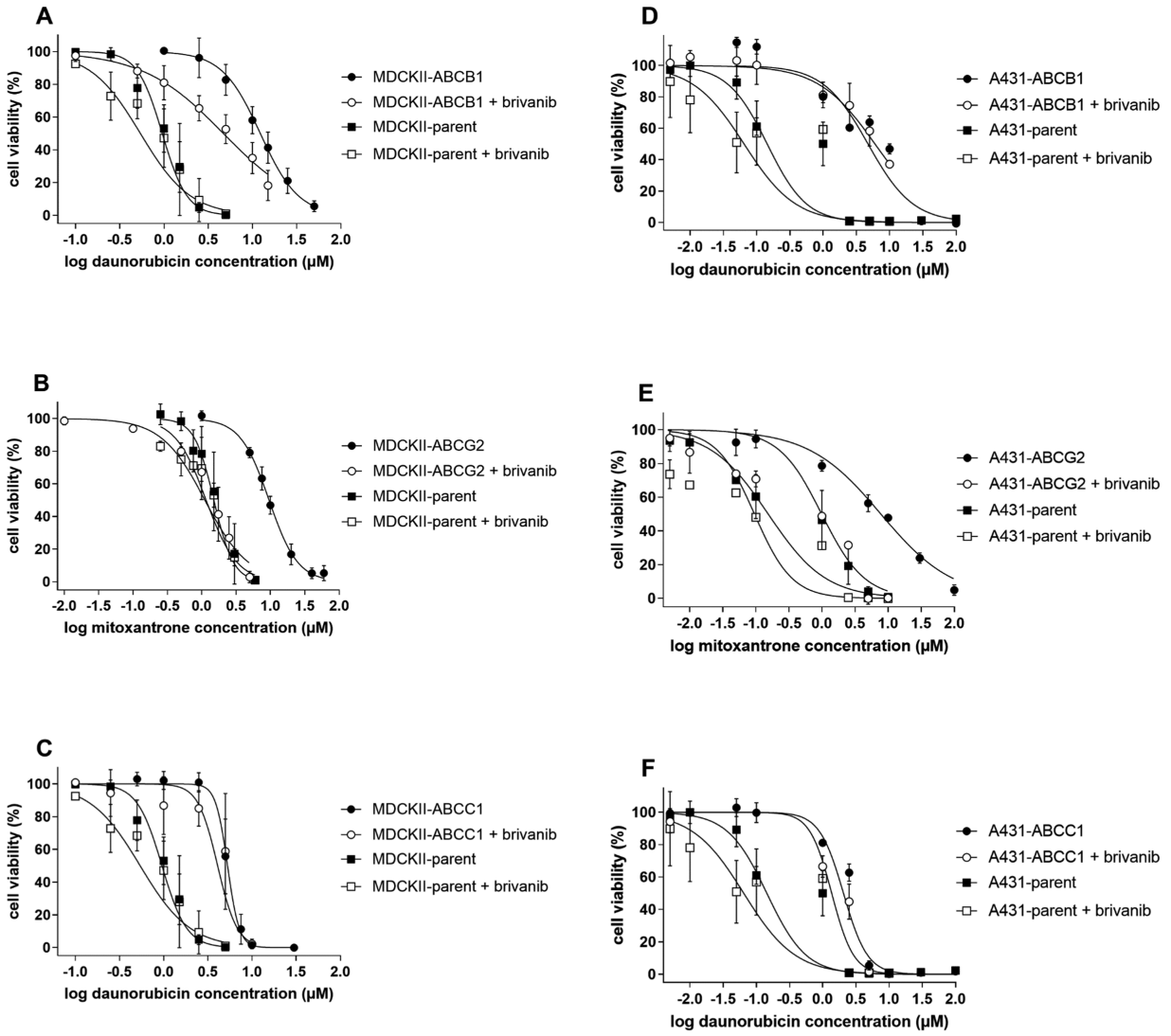

Figure 4. Effect of brivanib on the antiproliferative activities of daunorubicin or mitoxantrone in (A) MDCKII-ABCB1, (B) MDCKII-ABCG2, (C) MDCKII-ABCC1, (D) A431-ABCB1, (E) A431-ABCG2, and (F) A431-ABCC1 cells. Values obtained with parent cells are presented for each variant. The cells were treated with model cytotoxic drugs alone or in combination with 15 or 20 μM brivanib (mitoxantrone or daunorubicin combinations, respectively) for 48 h, and then cell proliferation was assessed by employing an MTT viability assay. Obtained results are subjected to subsequent analyses in Figure 5 and Table 1. The values are expressed as the mean ± SD of three independent experiments with biological triplicates in each repetition.

assessed to estimate the potential of brivanib to cause pharmacokinetic DDIs and modulate CYP3A4-mediated resistance to docetaxel. Brivanib strongly inhibited the CYP2B6, CYP2C19, CYP2C8, and CYP2C9 isoforms with IC_{50} values of 5.95, 3.64, 3.08, and 1.39 μM, respectively, and reached potencies comparable to the model inhibitors. Furthermore, low to moderate inhibitory activities were recorded for the CYP1A2, CYP3A4, and CYP2D6 isoenzymes (IC_{50} values of 44.5, 26.2, and 34.7 μM, respectively). Negligible level of interaction was observed for CYP3A5 (Figure 7).

3.6. Brivanib Does Not Affect CYP3A4 Metabolic Activity in Intact Cells. In these experiments, we aimed to confirm the potential of brivanib as a modulator of CYP3A4-mediated docetaxel resistance. However, in our HepG2-CYP3A4 cell-based assay, no CYP3A4 inhibition was observed at any of the brivanib concentrations; instead, a slight induction of enzyme activity was observed. In contrast, 10 μM of the model inhibitor ketoconazole reached 99.1% inhibition, demonstrating the validity of the method (Figure 8).

3.7. Effect of Brivanib on the mRNA Expression of Selected ABC Drug Efflux Transporters and CYP450 Isozymes. The upregulation of CYP450 isoenzymes and ABC transporters is another mechanism through which brivanib might influence the pharmacokinetics of simultaneously administered drugs. To explore this possible scenario, we investigated the effects of brivanib on the expression of *ABCB1*, *ABCG2*, *ABCC1*, *CYP1A2*, *CYP3A4*, and *CYP2B6* in the corresponding systemic cellular models (LS174T and Caco-2 cell lines, HepaFH3, and upcyte hepatocytes). Moreover, transporter-oriented gene expression studies were also performed in the NSCLC cell lines NCI-H1299 and A549 to estimate whether brivanib could influence resistance profile of one of its major target cells.

The selection of the brivanib concentration (i.e., 10 μM) followed two crucial rules: (1) the concentration exhibited negligible cytotoxicity in the tested cell lines (Figures 9A and

DOI: 10.1021/acs.molpharmaceut.9b00361
Mol. Pharmaceutics XXXX, XXX, XXX−XXX

Table 1. Detailed Analysis of the Co-treatment of MDCKII and A431 Cells with the Combinations of Brivanib with Chemotherapeutic Drugs

cell line	drug(s)[a]	IC_{50}[b] (μM)	95% CI (μM)	IC_{50} shift[c] (fold)
MDCKII-parent	daunorubicin	0.955	(0.750−1.23)	
	mitoxantrone	1.50	(1.24−1.85)	
	daunorubicin + brivanib	0.541[ns]	(0.388−0.733)	1.77
	mitoxantrone + brivanib	1.16[ns]	(0.871−1.57)	1.29
MDCKII-ABCB1	daunorubicin	12.3	(10.9−13.8)	
	daunorubicin + brivanib	4.70*	(3.85−5.82)	2.62
MDCKII-ABCG2	mitoxantrone	9.55	(8.80−10.4)	
	mitoxantrone + brivanib	1.11**	(0.754−1.72)	8.60
MDCKII-ABCC1	daunorubicin	5.29	(4.63−5.97)	
	daunorubicin + brivanib	4.09[ns]	(3.85−5.12)	1.29
A431-parent	daunorubicin	0.143	(0.0893−0.240)	
	mitoxantrone	0.154	(0.0565−1.50)	
	daunorubicin + brivanib	0.0644[ns]	(0.0261−0.137)	2.22
	mitoxantrone + brivanib	0.0952[ns]	(0.0752−0.116)	1.62
A431-ABCB1	daunorubicin	4.72	(2.51−8.40)	
	daunorubicin + brivanib	6.01[ns]	(4.56−7.46)	0.785
A431-ABCG2	mitoxantrone	7.77	(5.48−10.4)	
	mitoxantrone + brivanib	0.991*	(0.724−1.24)	7.84
A431-ABCC1	daunorubicin	2.05	(1.43−3.29)	
	daunorubicin + brivanib	1.37[ns]	(0.661−3.03)	1.50

[a]Brivanib at the concentration of 15 or 20 μM was combined with mitoxantrone or daunorubicin, respectively. [b]IC_{50} values were calculated from the curves depicted in Figure 4. The IC_{50} values of mitoxantrone or daunorubicin alone were compared to IC_{50} of their combinations with brivanib in particular cell sublines using the two-tailed unpaired *t*-test (*$p < 0.05$ and **$p < 0.01$). ns, not significant.. [c]IC_{50} shift values represent the ratio of IC_{50} of mitoxantrone or daunorubicin alone to IC_{50} of their combinations with brivanib within a particular cell subline.

10A) and (2) corresponded to plasma levels recorded in the patients with advanced or metastatic solid tumors.[29] Based on EMA guidance,[30] ABC transporter-related results were positive for induction (more than 100% change in mRNA level) only in the case of the *ABCB1* gene in the LS174T systemic model. The level of *ABCB1* induction evoked by brivanib was rather low, with fold-induction values of 2.54 and 2.09 compared to the model inducer rifampicin that reached fold-induction values of 5.94 and 4.89 after 24 and 48 h intervals, respectively (Figure 9B−E). In proliferating upcyte and HepaFH3 hepatocyte models, brivanib upregulated *CYP1A2* by 36.1- and 13.3-fold, although the induction potency was much lower compared to omeprazole, which caused 5703- and 1618-fold induction, respectively. Changes in *CYP2B6* and *CYP3A4* expression did not meet the criteria for induction/down-regulation in either of the cell lines (Figure 10B,C).

3.8. Brivanib Does Not Functionally Induce ABCB1 and CYP1A2. Herein, we aimed to evaluate the impact of mRNA changes that positively fit for induction according to EMA guidelines in previous experiments. Functional ABCB1 and CYP1A2 activity studies were employed in LS174T and HepaFH3/upcyte hepatocytes, respectively.

Competition between inhibition and induction is apparent from the ABCB1-oriented brivanib results. After 24 h, ABCB1 inhibition predominated, which was observed as a significant increase in rhodamine 123 accumulation by 24%. At 48 h, probe substrate accumulation was increased by 6% but without statistical significance. At 72 h, ABCB1 induction prevailed, which was observed as a 4% decrease in rhodamine 123 accumulation (Figure 11A). This observation is in accordance with protein induction as a long-lasting process; ABCB1 induction was not significantly manifested at the functional level as it was counterbalanced by inhibition throughout the experiment. Aware of the ABCB1-inhibitory properties of brivanib, we tried to evaluate the effect of drug withdrawal 6 h before activity assessment to eliminate transporter inhibition interference effects. Brivanib potentially maintained intracellular concentrations sufficient for transporter inhibition following withdrawal, as there were no significant differences between the data trends with or without brivanib washout (substrate accumulation increase by 21%, 0% change, and 6% decrease at 24, 48, and 72 h intervals, respectively). According to expectations, the model inducer rifampicin significantly decreased rhodamine 123 accumulation by 23, 30, and 38% at the 24, 48, and 72 h intervals, respectively (Figure 11A).

In HepaFH3 and upcyte hepatocytes, no significant increase in CYP1A2 activity was observed following 72 h exposure to brivanib. The model inducer omeprazole enhanced the metabolic function of CYP1A2 by 5.26- and 2.67-fold in HepaFH3 and upcyte hepatocytes (Figure 11B), respectively.

4. DISCUSSION

Brivanib is a promising tyrosine kinase inhibitor expected to enter the drug market for the treatment of solid tumors in China. While the pharmacodynamic behavior of this drug candidate has been described in a sufficient detail, its pharmacokinetic characteristics, especially interactions with drug-metabolizing enzymes and transporters, need to be addressed. In this study, we evaluated the possible interactions of brivanib with several ABC drug efflux transporters and CYP450 isoenzymes and aimed to address its potential for the modulation of pharmacokinetic MDR.

We first explored the possible inhibitory affinity of brivanib toward ABCG2, ABCB1, and ABCC1. While comparable trends were observed for ABCB1 and ABCG2, the inhibitory potencies varied by approximately 2-fold among fluorescent probe substrates and cytostatic model drugs. In our previous study focusing on the cyclin-dependent kinase inhibitor SNS-

DOI: 10.1021/acs.molpharmaceut.9b00361
Mol. Pharmaceutics XXXX, XXX, XXX−XXX

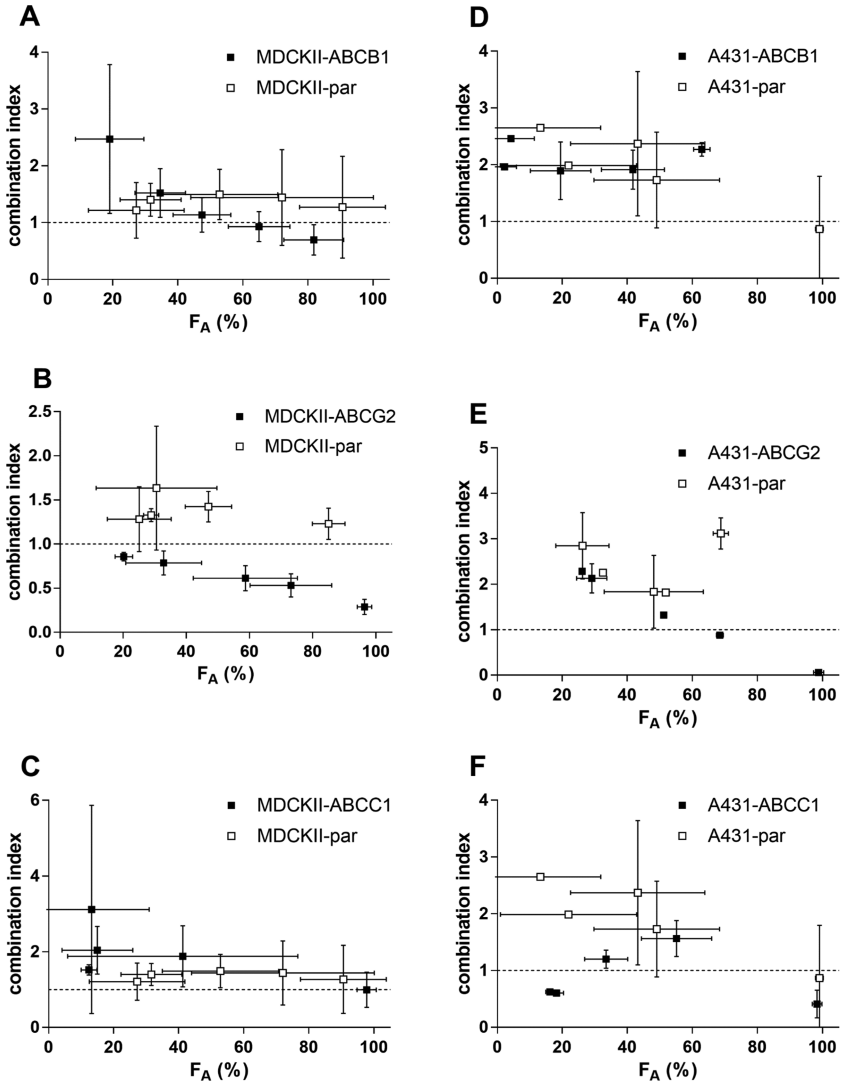

Figure 5. Quantification of the effects of combinations of brivanib with mitoxantrone or daunorubicin in MDCKII and A431 cells according to the combination index method. The data depicted in Figure 4 along with brivanib viability data (not shown) were subjected to median-effect analysis in the CompuSyn software. (A) Combination of brivanib with daunorubicin in MDCKII-ABCB1 or MDCKII-par cells, (B) combination of brivanib with mitoxantrone in MDCKII-ABCG2 or MDCKII-par cells, (C) combination of brivanib with daunorubicin in MDCKII-ABCC1 or MDCKII-par cells, (D) combination of brivanib with daunorubicin in A431-ABCB1 or A431-par cells, (E) combination of brivanib with mitoxantrone in A431-ABCG2 or A431-par cells, and (F) combination of brivanib with daunorubicin in A431-ABCC1 or A431-par cells. In Chou−Talalay's method, CI > 1.1 demonstrates an antagonism, CI > 0.9 and <1.1 shows an additivity, and CI < 0.9 determines a synergism. The data points are expressed as mean ± SD derived from three independent experiments with biological triplicates for each repetition.

032, we also observed similar variations.[19] Since ABC drug efflux transporters bear multiple substrate-binding sites that can be specific for particular model substrates,[31] our results suggest that brivanib probably affects the sites with a different degree of affinity. Based on our findings, the preferential affinity of substrates and inhibitors should be considered when performing transporter interaction studies since employing single substrates can eventually result in misleading interpretations. Importantly, only ABCG2 inhibitory activity of brivanib might potentially result in clinically relevant pharmacokinetic DDIs with respect to EMA/FDA guidelines,[30,32] the total C_{max} of 16.5 μM determined in patients with advanced or metastatic solid tumors[29] and the human plasma protein binding extent of 98.7%.[33] According to a basic model, in vitro hepatic interactions with efflux transporter systems can be considered potentially clinically relevant when the K_i (or IC_{50}) ≤ 50-fold unbound C_{max}. For intestinal interactions, possible clinical relevance is expected when I_{gut}/K_i (or IC50) ≥ 10, where I_{gut} = dose of inhibitor/250 mL.[30,32]

In the follow-up drug combination studies, we evaluated whether the observed inhibitory interactions could be utilized to reverse MDR to conventional drugs that are ABC transporter substrates. ABCG2 inhibition was clearly demonstrated to produce this effect in both MDCKII and A431 cellular models, whereas ABCB1 and especially ABCC1 participation in the modulation of MDR was questionable. This finding is in accordance with brivanib's inhibitory affinity toward particular transporters, where ABCG2 was most effectively inhibited followed by ABCB1 and ABCC1, and also conclusion concerning possible clinical relevance of observed transporter interactions mentioned above. In addition to the evaluation of the ability of brivanib to overcome MDR using IC_{50} shift analysis, we further aimed to exactly quantify outcomes of drug combinations in the

DOI: 10.1021/acs.molpharmaceut.9b00361
Mol. Pharmaceutics XXXX, XXX, XXX−XXX

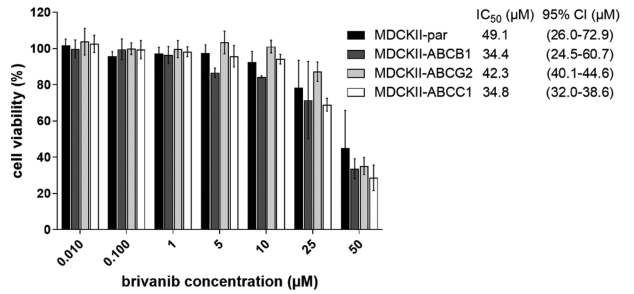

Figure 6. Comparison of cell sensitivity to brivanib in MDCKII-par and its transporter-overexpressing counterparts. The cells were treated with brivanib, and their proliferation was assessed by employing an MTT proliferation test following 48 h of incubation. Data were subjected to statistical analysis using one-way ANOVA followed by Dunnett's post hoc test. For each particular concentration, the viability values of the transporter-overexpressing cells were compared to those from parental cells; however, only insignificant differences were found at all of the points. Additionally, IC_{50} values were calculated and those from the transporter-overexpressing cells were compared to those from the parent cells using the two-tailed unpaired *t*-test, but only insignificant differences were found for all of the transporter-overexpressing sublines. Data are presented as mean ± SD from three independent experiments with biological triplicates for each repetition.

present work. In contrast to daunorubicin combination effects, which predominantly showed slight antagonism or additivity, strong synergism was observed in ABCG2-overexpressing cell lines over a significant portion of the F_A range. This is a crucial result as a synergism between drugs is hidden beyond the success of numerous chemotherapy regimens; it allows for the reduction of doses of simultaneously administered drugs, which dramatically increases the treatment safety and/or efficacy.[34] Limited information can be found regarding prospective combinations of brivanib with other antitumor agents. Recent preclinical studies employing various hepatocarcinoma cell lines or human lung cancer xenografts showed synergism for brivanib combinations with dasatinib or ixabepilone, respectively.[35,36] Furthermore, there are rational expectations that brivanib could overcome the pharmacodynamic resistance to doxorubicin that promoted by fibroblast growth factor receptor-mediated Raf-dependent survival signals.[37]

In addition to the characterization of brivanib as a chemosensitizer, we also aimed to explore its possible contrasting role in MDR, i.e., whether it can act as its victim. In our experiments, no significant differences in brivanib-induced antiproliferative effects were observed between parent and ABC transporter-overexpressing MDCKII cells. These results suggest that brivanib lacks high substrate affinity toward the examined transporters, and thus negligible effects of transporter functional expressions on tumor response to brivanib can be expected. In contrast to the prodrug brivanib alaninate (weak base, $pK_a \approx 7.6$), brivanib behaves as a very weak acid ($pK_a \approx 14.1$) with dramatically reduced ionizability and water solubility in organisms. Additionally, brivanib is a relatively highly lipophilic drug ($\log P \approx 2.9$) (calculated using Advanced Chemistry Development Software version 11.02). Based on both these properties, brivanib can readily penetrate biological membranes through passive diffusion. It is well known that physicochemical properties favoring drug passive diffusion, such as lipid solubility, are inversely correlated with its active transport by ABC drug efflux transporters.[38] In other

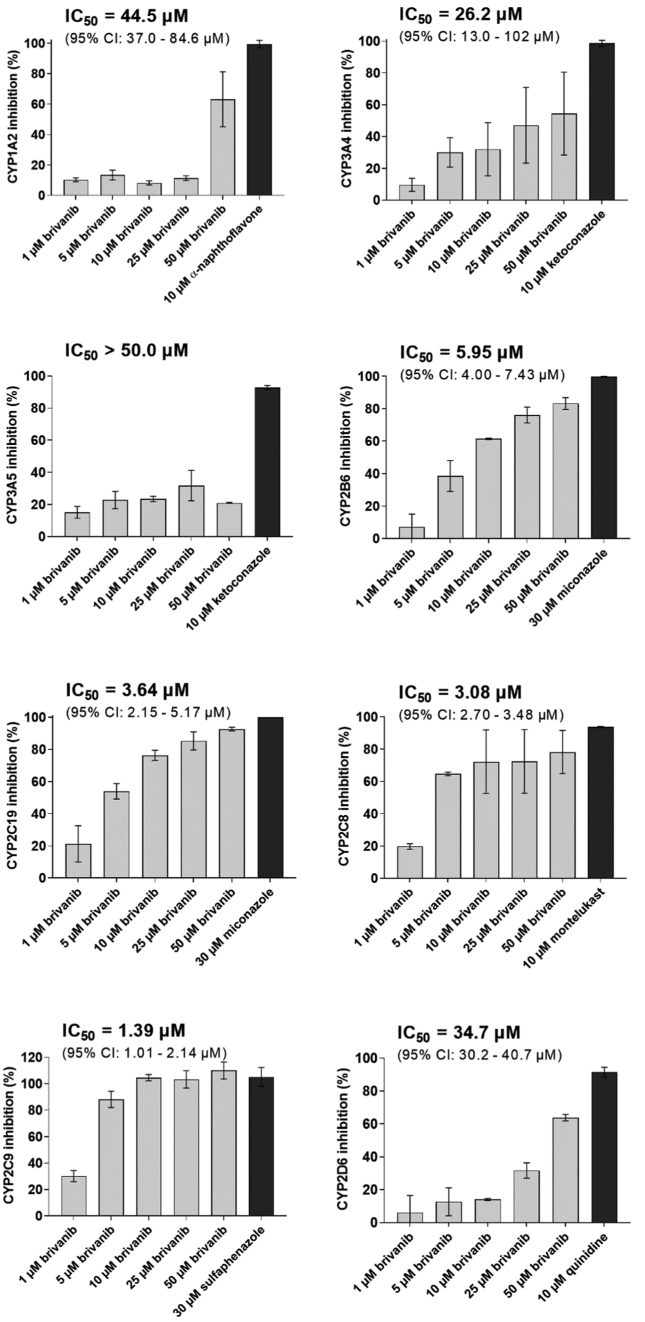

Figure 7. Effect of brivanib on the activities of human CYP1A2, CYP2B6, CYP2C8, CYP2C9, CYP2C19, CYP2D6, CYP3A4, or CYP3A5 determined using Vivid CYP450 screening kits. Brivanib and model inhibitors were preincubated with enzymes for 10 min, and then the reaction was started by the addition of a mixture of $NADP^+$ with a particular vivid substrate. Raw data from 15 min incubation intervals were normalized; the RFU values of variants with the enzyme and 0.5% DMSO were considered as the maximal (100%) enzyme activity. Fluorescence corresponding to 0% activity was obtained from samples incubated with the enzyme solvent buffer without enzyme and 0.5% DMSO. Data are presented as mean ± SD of three independent experiments with biological triplicate for each repetition.

words, moderate transporter-mediated efflux can be largely compensated for by passive membrane diffusion. These facts support the observed lack of the effect of ABCG2, ABCB1, and ABCC1 functional expression on the resistance to brivanib.

DOI: 10.1021/acs.molpharmaceut.9b00361
Mol. Pharmaceutics XXXX, XXX, XXX−XXX

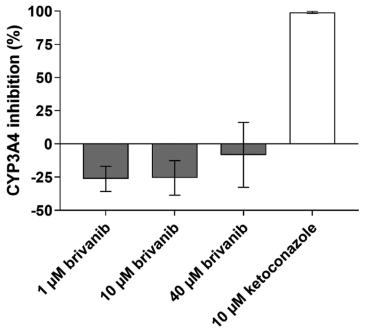

Figure 8. Effect of brivanib on human CYP3A4 metabolic activity in HepG2-CYP3A4 cells. The cells were preincubated with drugs for 10 min and then the reaction was started by the addition of luciferin-IPA substrate. After 45 min, the reaction was stopped and luminescence was assessed in the samples, which was followed by the determination of viability. Data from metabolic testing were normalized to viability values to compensate for possible inaccuracies caused by nonuniformity in cell growth or for false-positive results due to drug cytotoxicity. The resulting data were renormalized to % of inhibition. Data are expressed as mean ± SD of three independent experiments with biological triplicate for each repetition.

Our data introduce brivanib as a dual-mechanism drug whose modulatory capabilities are not impaired by the activities of any of MDR-associated ABC drug efflux transporters. In contrast, being both a transporter inhibitor and a high-affinity substrate, which is a disadvantageous feature of MDR modulators, is quite frequently seen for other tyrosine kinase inhibitors acting as dual-mechanism drugs.[39]

CYP3A4 constitutes an important mechanism for pharmacokinetic docetaxel resistance (unpublished data and refs 12−14 and 40). Therefore, it is of interest to further investigate the inhibitory activity of brivanib toward CYP3A4 to reveal its possible potential to attenuate this specific kind of resistance. Along with its role in resistance, CYP3A4 is also responsible for mediating a huge number of pharmacokinetic DDIs along with CYP1A2, CYP3A5, CYP2B6, CYP2C19, CYP2C8, CYP2C9, and CYP2D6;[30,32] these eight isoforms were included in testing to examine this additional issue. Considering the brivanib C_{max}[29] and the extent of plasma protein binding,[33] only CYP2C subfamily members and the CYB2B6 isoform could eventually become a clinically relevant site of brivanib-mediated DDIs, as shown in our results. Similar to hepatic efflux transporters, in vitro CYP450 inhibitory interactions are considered potentially clinically relevant when K_i (or IC_{50}) ≤ 50-fold unbound C_{max}.[30,32] Brivanib also partially inhibited recombinant CYP3A4, but this interaction was not confirmed at the cellular level. These results highlight the importance of cell-based or in vivo testing in enzymatic studies, as some substances may be potent inhibitors in an isolated system such as recombinant enzyme, but their biological activities in cells or tissues may be compromised by numerous factors (limited penetration through biological membranes, high cytotoxicity, efflux by transporters, metabolism by enzymes, sequestration into endosomes, etc.). Failure of brivanib inhibitory effects at the cellular level is in accordance with the reported lack of its effects on the pharmacokinetics of midazolam, a CYP3A4 substrate, in healthy subjects.[41]

In the final study, we examined the possible changes in ABC drug efflux transporter and CYP450 mRNA expression and activity in systemic and NSCLC models. With regard to our

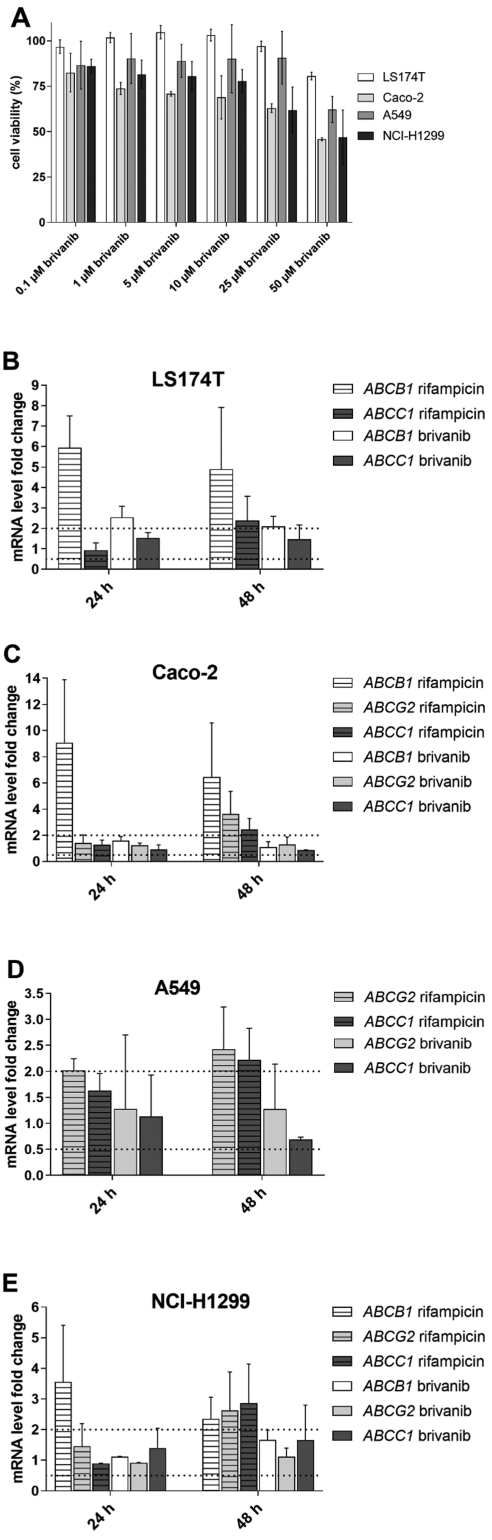

Figure 9. Changes in the expression of *ABCG2*, *ABCB1*, and *ABCC1* in (B, C) systemic and (D, E) NSCLC model cell lines following exposure to 10 μM brivanib. The brivanib concentration was chosen according to the (A) data from MTT assays and the brivanib C_{max}. In the gene expression studies, cell lines were incubated with 10 μM brivanib or 25 μM rifampicin and the mRNA levels of the examined genes were analyzed at 24 and 48 h intervals via quantitative real-time reverse transcription PCR. The analysis of the changes in mRNA levels of target genes was performed by employing the $2^{-\Delta\Delta Ct}$ method using the geometric mean of *B2M* and *HPRT1* values as an internal comparator. *ABCG2* and *ABCB1* were undetectable in LS174T and

DOI: 10.1021/acs.molpharmaceut.9b00361
Mol. Pharmaceutics XXXX, XXX, XXX−XXX

Figure 9. continued

A549 cells, respectively. The dotted lines define the boundaries of induction/downregulation positivity according to the recommendations given by drug regulatory authorities. Data are presented as mean ± SD of three independent experiments with biological triplicate for each repetition.

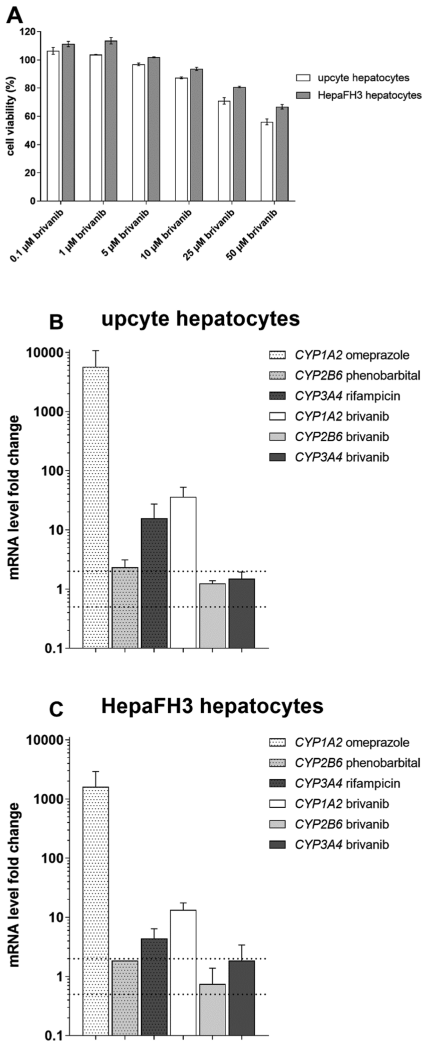

Figure 10. Effect of 10 μM brivanib on *CYP1A2*, *CYP2B6*, and *CYP3A4* mRNA levels in primary-like hepatocyte models derived from two different human donors: (B) upcyte and (C) HepaFH3 hepatocytes. The brivanib concentration was chosen based on the brivanib C_{max} and according to the (A) results of an ATP detection-based CellTiter Glo 2 viability assay. In the gene expression studies, the cells were incubated with 10 μM brivanib, 50 μM omeprazole, 750 μM phenobarbital, or 25 μM rifampicin and the mRNA levels of the examined genes were analyzed after 72 h via quantitative real-time reverse transcription PCR. The analysis of the changes in mRNA levels of target genes was performed with the $2^{-\Delta\Delta Ct}$ method using the geometric mean of *GAPDH* and *SDHA* values as an internal comparator. The dotted lines define the limits for induction/downregulation positivity according to the recommendations given by drug regulatory authorities. Data are expressed as mean ± SD of three independent experiments with biological triplicate for each repetition.

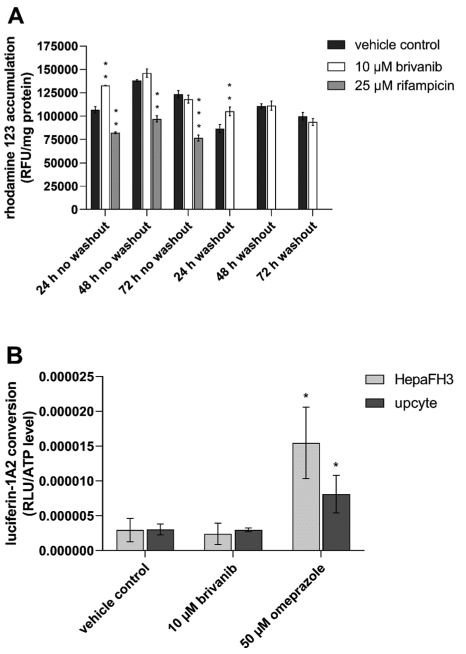

Figure 11. Changes in the activity of (A) ABCB1 in LS174T cells and (B) CYP1A2 in HepaFH3/upcyte hepatocytes following exposure to 10 μM brivanib. The cell lines were incubated with 10 μM brivanib or the respective model inducers, and the activity levels of examined proteins were analyzed using rhodamine 123 assay at 24, 48, and 72 h intervals (for ABCB1) or using a commercial P450-Glo CYP1A2 induction/inhibition assay at a 72 h interval (for CYP1A2). Raw activity data were normalized to protein contents or ATP levels. Normalized data were subjected to statistical analysis using the two-tailed unpaired *t*-test (*$p < 0.05$, **$p < 0.01$, and ***$p < 0.001$). Values of drug-treated samples were compared to the vehicle control values from a particular time interval (for ABCB1) or within a particular hepatocyte cell line (for CYP1A2). Values are expressed as mean ± SD of three independent experiments with biological triplicate for each repetition.

results, it is reasonable to anticipate that brivanib does not significantly affect the resistance profile of one of its target tumor cells and is not able to cause systemic drug–drug interactions due to the induction of CYP450 enzymes or ABC transporters. Since no significant *CYP3A4* induction has been observed, *CYP2C* subfamily members should also be insensitive to expression changes caused by brivanib (both subfamilies are co-induced following PXR nuclear receptor activation).[30,32] To date, no information is available regarding the effects of brivanib on the expression of ABC transporters and CYP450s playing role in drug resistance or DDIs.

In conclusion, we demonstrate brivanib as an inhibitor of ABCG2 and several CYP450 isoenzymes with potential to act as a perpetrator of clinically relevant pharmacokinetic DDIs. In addition, interactions with ABCG2 could be utilized for the attenuation of chemotherapeutic resistance, thus providing possible new therapeutic options for oncological patients. Of note, brivanib's modulatory abilities are not impaired by MDR-associated transporter efflux. We believe that the in vitro findings obtained in the present work might be used as an important background for subsequent in vivo investigations.

AUTHOR INFORMATION

Corresponding Author

*E-mail: jakub.hofman@faf.cuni.cz. Tel: +420-495067593. Fax: +420-495067170.

DOI: 10.1021/acs.molpharmaceut.9b00361
Mol. Pharmaceutics XXXX, XXX, XXX–XXX

ORCID

Jakub Hofman: 0000-0002-4285-7681
Simona Sucha: 0000-0001-9190-458X

Notes

The authors declare no competing financial interest.

■ ACKNOWLEDGMENTS

This work was supported by the Grant Agency of Charles University (project No. 1568218/C), by Charles University (SVV/2019/260-414), and by EFSA-CDN project (No. CZ.02.1.01/0.0/0.0/16_019/0000841) co-funded by ERDF. This publication was further supported by the European Funds for Regional Development (EFRE, Brandenburg, Germany; project "Entwicklung eines physiologisch relevanten Testsystems zur In-vitro-Erfassung von Hepatotoxizität im Hochdurchsatz", project No. 85009748). The authors declare no competing financial interests. This article is not an official guidance or policy statement of the U.S. Food and Drug Administration (FDA). No official support or endorsement by the U.S. FDA is intended or should be inferred.

■ ABBREVIATIONS

ABC, ATP-binding cassette; ABCB1, P-glycoprotein; ABCC1, multidrug resistance-associated protein 1; ABCG2, breast cancer resistance protein; CI, combination index; C_{max}, maximum plasma concentration; CYP450, cytochrome P450; DDI, drug−drug interaction; DMEM, Dulbecco's modified Eagle's medium; DMSO, dimethyl sulfoxide; EMA, European Medicines Agency; F_A, fraction of cells affected; FBS, fetal bovine serum; U.S. FDA, U.S. Food and Drug Administration; IC_{50}, half-maximal inhibitory concentration; MDCKII, Madin-Darby canine kidney subtype 2 cell line; MDR, multidrug resistance; MTT, 3-(4,5-dimethyl-2-thiazolyl)-2,5-diphenyl-2*H*-tetrazolium bromide; NSCLC, non-small cell lung cancer; PBS, phosphate-buffered saline; qRT-PCR, quantitative real-time reverse transcription PCR; RFU, relative fluorescence unit; SD, standard deviation

■ REFERENCES

(1) Wilson, L.; Bhatnagar, P.; Townsend, N. Comparing trends in mortality from cardiovascular disease and cancer in the United Kingdom, 1983-2013: joinpoint regression analysis. *Popul. Health Metrics* **2017**, *15*, No. 23.

(2) DeVita, V. T., Jr.; Chu, E. A history of cancer chemotherapy. *Cancer Res.* **2008**, *68*, 8643−8653.

(3) Chou, T.; Finn, R. S. Brivanib: a review of development. *Future Oncol.* **2012**, *8*, 1083−1090.

(4) Llovet, J. M.; Decaens, T.; Raoul, J. L.; Boucher, E.; Kudo, M.; Chang, C.; Kang, Y. K.; Assenat, E.; Lim, H. Y.; Boige, V.; Mathurin, P.; Fartoux, L.; Lin, D. Y.; Bruix, J.; Poon, R. T.; Sherman, M.; Blanc, J. F.; Finn, R. S.; Tak, W. Y.; Chao, Y.; Ezzeddine, R.; Liu, D.; Walters, I.; Park, J. W. Brivanib in patients with advanced hepatocellular carcinoma who were intolerant to sorafenib or for whom sorafenib failed: results from the randomized phase III BRISK-PS study. *J. Clin. Oncol.* **2013**, *31*, 3509−3516.

(5) Johnson, P. J.; Qin, S.; Park, J. W.; Poon, R. T.; Raoul, J. L.; Philip, P. A.; Hsu, C. H.; Hu, T. H.; Heo, J.; Xu, J.; Lu, L.; Chao, Y.; Boucher, E.; Han, K. H.; Paik, S. W.; Robles-Avina, J.; Kudo, M.; Yan, L.; Sobhonslidsuk, A.; Komov, D.; Decaens, T.; Tak, W. Y.; Jeng, L. B.; Liu, D.; Ezzeddine, R.; Walters, I.; Cheng, A. L. Brivanib versus sorafenib as first-line therapy in patients with unresectable, advanced hepatocellular carcinoma: results from the randomized phase III BRISK-FL study. *J. Clin. Oncol.* **2013**, *31*, 3517−3524.

(6) Ye, S. L.; Chen, X.; Yang, J.; Bie, P.; Zhang, S.; Liu, F.; Liu, L.; Zhou, J.; Dou, K.; Yip, C. S.; Yang, X. Evaluation of sorafenib in Chinese unresectable hepatocellular carcinoma patients with prior surgery and portal vein tumor thrombosis: A subset analysis of GIDEON study data. *Tumour Biol.* **2017**, *39*, No. 1010428317695030.

(7) Szakács, G.; Váradi, A.; Özvegy-Laczka, C.; Sarkadi, B. The role of ABC transporters in drug absorption, distribution, metabolism, excretion and toxicity (ADME-Tox). *Drug Discovery Today* **2008**, *13*, 379−393.

(8) Zanger, U. M.; Schwab, M. Cytochrome P450 enzymes in drug metabolism: regulation of gene expression, enzyme activities, and impact of genetic variation. *Pharmacol. Ther.* **2013**, *138*, 103−141.

(9) Prueksaritanont, T.; Chu, X.; Gibson, C.; Cui, D.; Yee, K. L.; Ballard, J.; Cabalu, T.; Hochman, J. Drug-drug interaction studies: regulatory guidance and an industry perspective. *AAPS J.* **2013**, *15*, 629−645.

(10) Fletcher, J. I.; Haber, M.; Henderson, M. J.; Norris, M. D. ABC transporters in cancer: more than just drug efflux pumps. *Nat. Rev. Cancer* **2010**, *10*, 147−156.

(11) Robey, R. W.; Pluchino, K. M.; Hall, M. D.; Fojo, A. T.; Bates, S. E.; Gottesman, M. M. Revisiting the role of ABC transporters in multidrug-resistant cancer. *Nat. Rev. Cancer* **2018**, *18*, 452−464.

(12) Michael, M.; Doherty, M. M. Tumoral drug metabolism: overview and its implications for cancer therapy. *J. Clin. Oncol.* **2005**, *23*, 205−229.

(13) Rochat, B. Importance of influx and efflux systems and xenobiotic metabolizing enzymes in intratumoral disposition of anticancer agents. *Curr. Cancer Drug Targets* **2009**, *9*, 652−674.

(14) Vadlapatla, R. K.; Vadlapudi, A. D.; Pal, D.; Mitra, A. K. Mechanisms of drug resistance in cancer chemotherapy: coordinated role and regulation of efflux transporters and metabolizing enzymes. *Curr. Pharm. Des.* **2013**, *19*, 7126−7140.

(15) Bugde, P.; Biswas, R.; Merien, F.; Lu, J.; Liu, D. X.; Chen, M.; Zhou, S.; Li, Y. The therapeutic potential of targeting ABC transporters to combat multi-drug resistance. *Expert Opin. Ther. Targets* **2017**, *21*, 511−530.

(16) Kathawala, R. J.; Gupta, P.; Ashby, C. R., Jr.; Chen, Z. S. The modulation of ABC transporter-mediated multidrug resistance in cancer: a review of the past decade. *Drug Resist. Updates* **2015**, *18*, 1−17.

(17) Beretta, G. L.; Cassinelli, G.; Pennati, M.; Zuco, V.; Gatti, L. Overcoming ABC transporter-mediated multidrug resistance: The dual role of tyrosine kinase inhibitors as multitargeting agents. *Eur. J. Med. Chem.* **2017**, *142*, 271−289.

(18) Hofman, J.; Ahmadimoghaddam, D.; Hahnova, L.; Pavek, P.; Ceckova, M.; Staud, F. Olomoucine II and purvalanol A inhibit ABCG2 transporter in vitro and in situ and synergistically potentiate cytostatic effect of mitoxantrone. *Pharmacol. Res.* **2012**, *65*, 312−319.

(19) Cihalova, D.; Hofman, J.; Ceckova, M.; Staud, F. Purvalanol A, olomoucine II and roscovitine inhibit ABCB1 transporter and synergistically potentiate cytotoxic effects of daunorubicin in vitro. *PLoS One* **2013**, *8*, No. e83467.

(20) Cihalova, D.; Ceckova, M.; Kucera, R.; Klimes, J.; Staud, F. Dinaciclib, a cyclin-dependent kinase inhibitor, is a substrate of human ABCB1 and ABCG2 and an inhibitor of human ABCC1 in vitro. *Biochem. Pharmacol.* **2015**, *98*, 465−472.

(21) Cihalova, D.; Staud, F.; Ceckova, M. Interactions of cyclin-dependent kinase inhibitors AT-7519, flavopiridol and SNS-032 with ABCB1, ABCG2 and ABCC1 transporters and their potential to overcome multidrug resistance in vitro. *Cancer Chemother. Pharmacol.* **2015**, *76*, 105−116.

(22) Sorf, A.; Hofman, J.; Kucera, R.; Staud, F.; Ceckova, M. Ribociclib shows potential for pharmacokinetic drug-drug interactions being a substrate of ABCB1 and potent inhibitor of ABCB1, ABCG2 and CYP450 isoforms in vitro. *Biochem. Pharmacol.* **2018**, *154*, 10−17.

(23) Elkind, N. B.; Szentpetery, Z.; Apati, A.; Ozvegy-Laczka, C.; Varady, G.; Ujhelly, O.; Szabo, K.; Homolya, L.; Varadi, A.; Buday, L.; Keri, G.; Nemet, K.; Sarkadi, B. Multidrug transporter ABCG2

DOI: 10.1021/acs.molpharmaceut.9b00361
Mol. Pharmaceutics XXXX, XXX, XXX−XXX

prevents tumor cell death induced by the epidermal growth factor receptor inhibitor Iressa (ZD1839, Gefitinib). *Cancer Res.* **2005**, *65*, 1770−1777.
(24) Xuan, J.; Chen, S.; Ning, B.; Tolleson, W. H.; Guo, L. Development of HepG2-derived cells expressing cytochrome P450s for assessing metabolism-associated drug-induced liver toxicity. *Chem. Biol. Interact.* **2016**, *255*, 63−73.
(25) Herzog, N.; Hansen, M.; Miethbauer, S.; Schmidtke, K. U.; Anderer, U.; Lupp, A.; Sperling, S.; Seehofer, D.; Damm, G.; Scheibner, K.; Kupper, J. H. Primary-like human hepatocytes genetically engineered to obtain proliferation competence display hepatic differentiation characteristics in monolayer and organotypical spheroid cultures. *Cell Biol. Int.* **2016**, *40*, 341−353.
(26) Ramachandran, S. D.; Vivares, A.; Klieber, S.; Hewitt, N. J.; Muenst, B.; Heinz, S.; Walles, H.; Braspenning, J. Applicability of second-generation upcyte(R) human hepatocytes for use in CYP inhibition and induction studies. *Pharmacol. Res. Perspect.* **2015**, *3*, No. e00161.
(27) Hofman, J.; Sorf, A.; Vagiannis, D.; Sucha, S.; Novotna, E.; Kammerer, S.; Kupper, J. H.; Ceckova, M.; Staud, F. Interactions of Alectinib with Human ATP-Binding Cassette Drug Efflux Transporters and Cytochrome P450 Biotransformation Enzymes: Effect on Pharmacokinetic Multidrug Resistance. *Drug Metab. Dispos.* **2019**, *47*, 699−709.
(28) Chou, T. C. Theoretical basis, experimental design, and computerized simulation of synergism and antagonism in drug combination studies. *Pharmacol. Rev.* **2006**, *58*, 621−681.
(29) Mekhail, T.; Masson, E.; Fischer, B. S.; Gong, J.; Iyer, R.; Gan, J.; Pursley, J.; Patricia, D.; Williams, D.; Ganapathi, R. Metabolism, excretion, and pharmacokinetics of oral brivanib in patients with advanced or metastatic solid tumors. *Drug Metab. Dispos.* **2010**, *38*, 1962−1966.
(30) EMA. *Guideline on the Investigation of Drug Interactions*, CPMP/EWP/560/95/Rev. 1 Corr. 2**; European Medicines Agency, 2012.
(31) Szöllősi, D.; Rose-Sperling, D.; Hellmich, U. A.; Stockner, T. Comparison of mechanistic transport cycle models of ABC exporters. *Biochim. Biophys. Acta, Biomembr.* **2018**, *1860*, 818−832.
(32) FDA. In Vitro Metabolism- and Transporter-Mediated Drug−Drug Interaction Studies Guidance for Industry. *Clinical Pharmacology*; CDER: Silver Spring, 2017.
(33) Marathe, P. H.; Kamath, A. V.; Zhang, Y.; D'Arienzo, C.; Bhide, R.; Fargnoli, J. Preclinical pharmacokinetics and in vitro metabolism of brivanib (BMS-540215), a potent VEGFR2 inhibitor and its alanine ester prodrug brivanib alaninate. *Cancer Chemother. Pharmacol.* **2009**, *65*, 55−66.
(34) Bayat Mokhtari, R.; Homayouni, T. S.; Baluch, N.; Morgatskaya, E.; Kumar, S.; Das, B.; Yeger, H. Combination therapy in combating cancer. *Oncotarget* **2017**, *8*, 38022−38043.
(35) Chang, A. Y.; Wang, M. In-vitro growth inhibition of chemotherapy and molecular targeted agents in hepatocellular carcinoma. *Anticancer Drugs* **2013**, *24*, 251−259.
(36) Lee, F.; Jure-Kunkel, M. N.; Salvati, M. E. Synergistic activity of ixabepilone plus other anticancer agents: preclinical and clinical evidence. *Ther. Adv. Med. Oncol.* **2011**, *3*, 11−25.
(37) Alavi, A.; Hood, J. D.; Frausto, R.; Stupack, D. G.; Cheresh, D. A. Role of Raf in vascular protection from distinct apoptotic stimuli. *Science* **2003**, *301*, 94−96.
(38) Cygalova, L. H.; Hofman, J.; Ceckova, M.; Staud, F. Transplacental pharmacokinetics of glyburide, rhodamine 123, and BODIPY FL prazosin: effect of drug efflux transporters and lipid solubility. *J. Pharmacol. Exp. Ther.* **2009**, *331*, 1118−1125.
(39) Deng, J.; Shao, J.; Markowitz, J. S.; An, G. ABC transporters in multi-drug resistance and ADME-Tox of small molecule tyrosine kinase inhibitors. *Pharm. Res.* **2014**, *31*, 2237−2255.
(40) Miyoshi, Y.; Ando, A.; Takamura, Y.; Taguchi, T.; Tamaki, Y.; Noguchi, S. Prediction of response to docetaxel by CYP3A4 mRNA expression in breast cancer tissues. *Int. J. Cancer* **2002**, *97*, 129−132.
(41) Syed, S.; Clemens, P. L.; Lathers, D.; Kollia, G.; Dhar, A.; Walters, I.; Masson, E. Lack of effect of brivanib on the pharmacokinetics of midazolam, a CYP3A4 substrate, administered intravenously and orally in healthy participants. *J. Clin. Pharmacol.* **2012**, *52*, 914−921.

DOI: 10.1021/acs.molpharmaceut.9b00361
Mol. Pharmaceutics XXXX, XXX, XXX−XXX